Arabian Journal of Chemistry (2022) **15**, 103926

King Saud University

Arabian Journal of Chemistry

www.ksu.edu.sa
www.sciencedirect.com

ORIGINAL ARTICLE

Performance of dodecyl dimethyl benzyl ammonium chloride as bactericide and corrosion inhibitor for 7B04 aluminum alloy in an aircraft fuel system

Shuai Wang [a], Jie Sun [b], Borong Shan [c], Weijie Fan [c,*], Rui Ding [a], Jie Yang [a], Xiaodong Zhao [a,*]

[a] *School of Ocean, Yantai University, Yantai 264005, China*
[b] *Fisheries College, Ocean University of China, Qingdao 266100, China*
[c] *Qingdao Campus of Naval Aeronautical University, Qingdao 266041, China*

Received 10 February 2022; accepted 13 April 2022
Available online 21 April 2022

KEYWORDS

Dodecyl dimethyl benzyl ammonium chloride;
Bactericide;
Electrochemistry;
Corrosion inhibitor;
Quantum chemical calculations

Abstract In this study, the broad-spectrum antimicrobial property of dodecyl dimethyl benzyl ammonium chloride (DDBAC) was investigated against three species of bacteria, *Lysinibacillus sphaericus* (*L. sphaericus*), *Acinetobacter lwoffii* (*A. lwoffii*), and *Sediminibacterium salmoneum* (*S. salmoneum*) isolated and purified from a naval aircraft fuel system. Through the inhibition zone method and minimum inhibitory concentration test, DDBAC was found to have a good antimicrobial performance with a minimum inhibitory concentration of 64 mg/L. The influence of DDBAC on the corrosion behavior of fuel tank material was evaluated by electrochemical measurements, such as polarization curve and electrochemical impedance spectroscopy (EIS). The polarization curve indicated that DDBAC suppressed anodic and cathodic reactions as a mixed-type corrosion inhibitor, and the inhibition efficiency was 68.38% at the concentration of 80 mg/L after 28 days of immersion. The EIS results showed that DDBAC inhibited the corrosion of 7B04 aluminum alloy in the concentration range of 40–120 mg/L. The DDBAC adsorption on the aluminum alloy surface was in agreement with the modified Langmuir adsorption isotherm model. The quantum chemical calculations proved that a lone pair of electrons of nitrogen atoms in DDBAC were able to form coordinate bonds with the empty orbital in aluminum, resulting in a tight chemisorption layer on the aluminum alloy surface and corrosion inhibition.

* Corresponding authors.
E-mail addresses: fanweijie520@qq.com (W. Fan), zhaoxiaodong23@163.com (X. Zhao).

Peer review under responsibility of King Saud University.

Production and hosting by Elsevier

1. Introduction

The naval aircraft corrosion is a problem that every country needs to face in a harsh environment (Li et al., 2012). Specifically, for the carrier-based aircraft moored on the aircraft carrier, in addition to the high temperature, high humidity, and high salt condition, the splash of waves and weak acidic exhaust emissions from the aircraft

https://doi.org/10.1016/j.arabjc.2022.103926
1878-5352

carrier and aircraft engines make the service environment severe. As service time increases, corrosion problems of aircraft fuselages arise frequently, and some even endanger flight safety, and many aircraft have to be grounded for repairs (Pantelakis et al., 2012).

The vital function of the aircraft fuel system is to store aviation fuel and ensure the regular operation of the engine with a sequential fuel supply (Brown et al., 2010). Therefore, the cleanliness of aviation fuel is directly related to the flight safety of the aircraft. Microbial contamination in aviation fuel, due to its insidious and unavoidable nature, has become a major problem in fuel contamination and material corrosion. It has also attracted the increasing attention of researchers (Passman, 2013; Bücker et al., 2014). Therefore, investigating the inhibition of microbial contamination of aviation fuel is of great importance.

The addition of bactericides is currently considered to be an effective measure for the prevention of microbial contamination (Liu et al., 2020). Bactericides kill or inhibit microorganisms by affecting their morphology, composition, metabolism, and physiological activities (Cui et al., 2021). Many types of bactericides have been widely used in various fields, but only a few of them are suitable for aviation fuel systems (Wang et al., 2019). The reason is that bactericides for aviation fuel must meet considerable requirements, such as good broad-spectrum activity, chemical stability, and cost effectiveness (Finšgar and Jackson, 2014). Most importantly, the bactericides themselves should not accelerate the corrosion of the fuel system materials to avoid further damage.

Quaternary ammonium compounds are probably the best chemicals to inhibit microbial germination (Jennings et al., 2015). They have been widely used in various fields, such as food, medicine, oil field and industrial water treatment, owing to their broad antibacterial spectrum, good water solubility and environmental stability (Gu et al., 2018; Zhang et al., 2018; Shi et al., 2020). Antimicrobial agents, such as Cl, ClO_2, and O_3, usually cause environmental pollution (Deyab, 2018). In comparison, quaternary ammonium molecules provide a safe way by increasing antimicrobial activity and reducing dual pollution (Xue et al., 2015).

The mechanism of quaternary ammonium salts as bactericides has also been intensively studied (Ding et al., 2011; Zhu et al., 2015a,b). The active agent on the bactericide surface penetrates the bacterial cell membrane by electrostatic gravity to cause the internal substances leaking out and eventually results in cell lysis and death (Zhang et al., 2020a,b; Samy et al., 2015). In addition, some quaternary ammonium bactericides have corrosion inhibition properties (Zhu et al., 2016).

Dodecyl dimethyl benzyl ammonium chloride (DDBAC) is a kind of quaternary ammonium compound with broad-spectrum and highly effective antimicrobial ability (Shi et al., 2020). It is also a cationic surfactant. Surfactant is commonly used as a corrosion inhibitor for the corrosion protection of metal materials (Karn et al., 2017; Verma et al., 2020). The amphiphilicity of surfactant molecules creates an affinity for adsorption at interfaces such as the metal/metal oxide–water interface (Abd-Elaal et al., 2017). Surfactants adsorb on the metal and metal oxide surfaces to form a barrier that prevents the exposure of the active sites to the corrosive medium and thereby reduces corrosion (Migahed et al., 2012; Krishnaveni and Ravichandran, 2014; Tan et al., 2021; Samy et al., 2015). The presence of specific atoms, such as N and O, in these compounds plays an important role in determining the adsorption mechanism and corrosion inhibition efficiency (Zhu et al., 2015a,b). Although several studies have been reported in the literature on the use of quaternary ammonium compounds as antimicrobial agents and corrosion inhibitors, the effect of DDBAC on microorganisms in aircraft fuel systems has almost hardly been involved.

In this study, the microorganisms used in the experiments were all extracted from naval aircraft fuel systems in previous work (Wang et al., 2022). The broad-spectrum antimicrobial property of DDBAC against three representative bacteria, *Lysinibacillus sphaericus* (*L. sphaericus*), *Acinetobacter lwoffii* (*A. lwoffii*), and *Sediminibacterium salmoneum* (*S. salmoneum*) was investigated using the inhibition zone method and minimum inhibitory concentration test. Taking *L. sphaericus* as an example, the influence of DDBAC on the corrosion of fuel tank material was evaluated by polarization curve and electrochemical impedance spectroscopy (EIS). The adsorption mechanism of DDBAC on the aluminum alloy surface was discussed through quantum chemical calculations and density functional theory (DFT) calculations.

2. Experimental

2.1. Materials

The fuel sample was taken from a naval aircraft fuel system. Three strains of *L. sphaericus, A. lwoffii*, and *S. Salmoneum* were isolated and selected for this study. The Luria-Bertani (LB) medium was used for the bacteria culture. The purity of DDBAC was 95%, provided by Shanghai McLean Biochemical Reagent Co., Ltd.

The main chemical compositions of the 7B04 aluminum alloy in the experiment were Ni (less than0.1%), Ti (0.05–0.4%), Si (0.3%), Cu (3.2–3.7%), Zn (0.1%), Mg (2.1–2.6%), Mn (0.50–0.80%), Fe (0.3%), and Al balance. The 7B04 aluminum alloy sample was processed into a sheet of 10 mm × 10 mm × 2 mm. The working face of the sample was cut with a square working area of 1 cm^2, and the non-working surface was welded with a copper wire and then sealed with epoxy resin and ethylenediamine. Before the experiment, the sample was polished with 800 to 2000 # sandpapers, rinsed with distilled water and degreased with acetone.

Fig. 1 shows the chemical structure and optimized structure of DDBAC.

2.2. Bacteriostatic test

Three strains of bacteria were cultured for 20 h in a constant temperature shaker at a speed of 170 r/min at 37 °C (Sylvie and Pierre, 2012). The concentration of the bacteria medium was adjusted to 5×10^5–5×10^6 cfu/ml with sterile diluted water, so the absorbance values measured by the ultraviolet spectrophotometer at 600 nm ranged between 0.800–1.000. The bacterial suspension and the culture medium were mixed at a ratio of 15 μl: 25 μl, and then added to a culture plate for condensation. After the medium solidification, three holes with a 2 mm diameter were punched in each culture plate and filled with 10 μl bactericide. The DDBAC concentrations were 40, 60, 80, 100 and 120 mg/L, respectively. The culture plate was placed in a constant temperature incubator at 37 °C for 20 h, and then the diameter of the bacteriostatic zone was measured.

2.3. Minimum inhibitory concentration

The 10 μl of bacterial suspension was added to wells 1–11 of a 96-well plate and 85 μl of sterile medium was added to wells 1–10. The 90 μl of the sterile liquid medium was added to well 11 as a positive control (PC) and 100 μl of the sterile liquid medium into well 12 as a negative control (NC). The bactericide was serially diluted from 256 mg/mL to 1 mg/mL by using the double dilution method. Wells 1–10 were filled with 5 μl of bactericide in order of concentration with three parallel groups of each concentration. These wells were then cultured

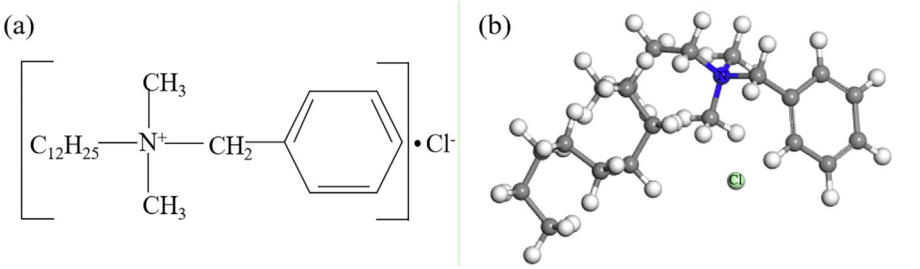

Fig. 1 Chemical structure (a) and optimized structure (b) of DDBAC.

in an incubator at 37 °C for 20 h. Finally, 10 µl of resazurin with a concentration of 1 mg/mL was added to wells 1–11, and the color change of the indicator was observed (Chowdhuri et al., 2017).

2.4. Electrochemical measurements

The electrochemical workstation (PARSTAT2273, USA) was used for electrochemical analysis. A three-electrode system was used, with 7B04 aluminum alloy as the working electrode, Pt electrode as the auxiliary electrode, and saturated calomel electrode (SCE) as the reference electrode. The open circuit potential was measured in a 3.5% NaCl solution with DDBAC concentrations of 40, 60, 80, 100, and 120 mg/L and a blank system without DDBAC. EIS was carried out in the frequency range from 10^{-2} to 10^{5} Hz, and the sinusoidal voltage signal was 10 mV (Liu et al., 2017). The data were processed using ZSimpWin software to analyze the structure of the equivalent circuit and the parameters of the components. The electrochemical polarization curve was scanned with a scanning rate of 0.333 mV/s and a range of ±350 mV relative to the open circuit potential. Furthermore, the data were analyzed by C-view software.

2.5. Quantum chemical study

Quantum chemical studies were defined by Materials Studio software based on DFT. The molecular structure was optimized using the Dmol 3 module in the software (Shaban et al., 2015). The PBE functional under the generalized gradient approximation (GGA) was chosen for the structure optimization process. After structure optimization, the DDBAC molecule was calculated. The quantum chemical parameters computed included the lowest unoccupied molecular orbital energy (E_{LUMO}), the highest occupied molecular orbital energy (E_{HOMO}), energy gap ($\Delta E = E_{LUMO} - E_{HOMO}$), Mulliken atomic charge distribution, and molecular electrostatic potential (MEP).

3. Results

3.1. Bacteriostatic test

Fig. 2 shows the bacterial inhibitory activity at different DDBAC concentrations against *L. sphaericus*, *S. salmoneum*, and *A. lwoffii*. The antibacterial ability of DDBAC against the three species of bacteria was evaluated using the inhibition zone method. The experimental results revealed that *S. salmoneum*, *A. lwoffii*, and *L. sphaericus* were inhibited when the DDBAC concentration reached 60 mg/L, and the DDBAC had the best inhibitory effect on *A. lwoffii* at all concentrations. The above analysis showed that DDBAC was a broad-spectrum and effective bactericide for inhibiting microbial growth in an aircraft fuel system.

3.2. Minimum inhibitory concentration

In this study, the critical point of the minimum inhibitory concentration was determined by the resazurin indicator. It is shown as blue when the bactericide has antibacterial activity, and pink or white color indicated weak or no antibacterial activity. Therefore, the minimum inhibitory concentration could be determined according to the color change. As illustrated in Fig. 3, the minimum inhibitory concentration of DDBAC was 64 mg/L.

3.3. Polarization measurements

The bactericide should not accelerate the corrosion of aircraft fuel system material to avoid further damage. In the aerospace industry, high-strength aluminum alloys, such as Al 7B04, are still the preferred material for manufacturing different structural components. Therefore, the influence of DDBAC on the corrosion of aluminum alloy was investigated by electro-

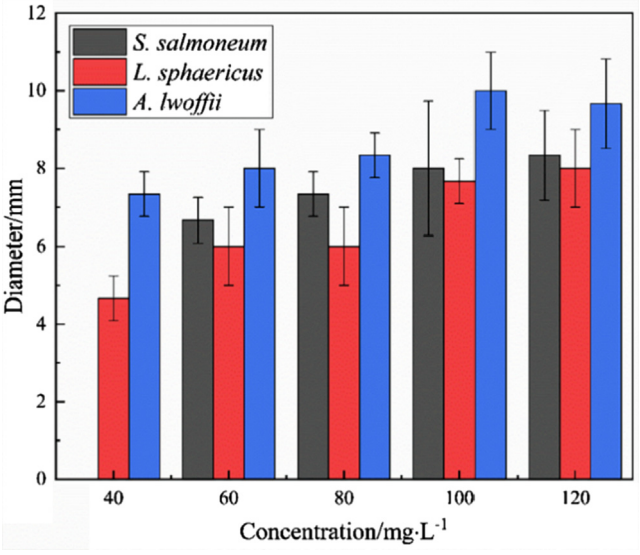

Fig. 2 Inhibitory results of DDBAC.

chemical experiments. Fig. 4 shows the polarization curve of 7B04 aluminum alloy immersed in different systems for 28 days. The Tafel zone corresponding to the polarization curve was linearly fitted, and the electrochemical corrosion parameters obtained are presented in Table 1.

Table 1 also shows that i_{corr} decreased in the presence of DDBAC, indicating that the DDBAC had an inhibitory effect on the corrosion of 7B04 aluminum alloy. With the addition of DDBAC, E_{corr} changed slightly. However, if the displacement of E_{corr} in the presence of an inhibitor compared with the blank solution is more than ±85 mV/SCE, then the inhibitor is classified as cathodic or anodic type (Hsissou et al., 2020). The maximum displacement in this study was less than 48 mV/SCE, indicating that DDBAC acts as a mixed-type inhibitor. The inhibition efficiency (η) is defined as:

$$\eta = \frac{I^{o}_{corr} - I_{corr}}{I^{o}_{corr}} \times 100 \quad (1)$$

where I^{0}_{corr} and i_{corr} represent corrosion current density values without and with inhibitor, respectively.

The values calculated from Eq. (1) are shown in Table 1. When the DDBAC concentration was 60–120 mg/L, the inhibition efficiency was over 60%. The maximum inhibitory efficiency was obtained at 80 mg/L (68.38%).

3.4. EIS measurements

Fig. 5 illustrates the Nyquist and Bode plots of 7B04 aluminum alloys immersed in systems with different DDBAC concentrations.

As shown in Fig. 5(a), after 21 days of immersion, the radius of the capacitive resistance arc of each system with the addition of different DDBAC concentrations was larger than that of the blank system. The increase in the Nyquist diameter could be attributed to the protection given by DDBAC molecules. These data proved the DDBAC adsorption on the aluminum alloy surface (Yadav et al., 2016). Moreover, the addition of 60 mg/L DDBAC had the best corrosion inhibition effect on aluminum alloy. In Fig. 5(c), the capacitive reactance arc radius of 60 mg/L DDBAC increased with time. It indicated that the corrosion of the aluminum alloy was inhibited by 60 mg/L DDBAC throughout the 21 days.

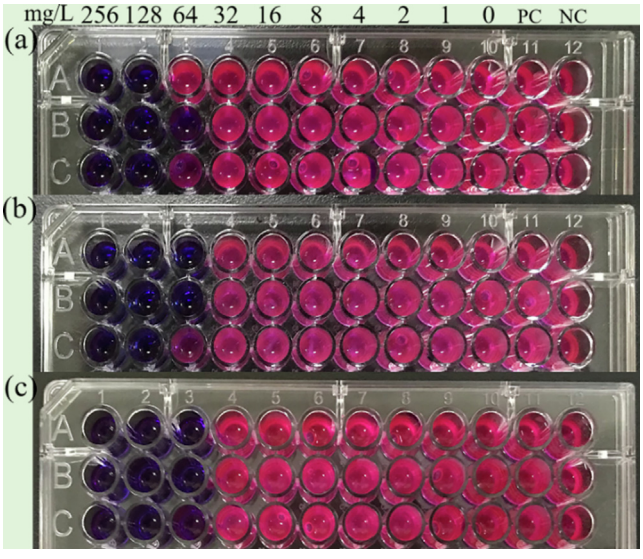

Fig. 3 Minimum inhibitory concentration results of DDBAC against *S. salmoneum*(a), *L. sphaericus*(b), and *A. lwoffii*(c).

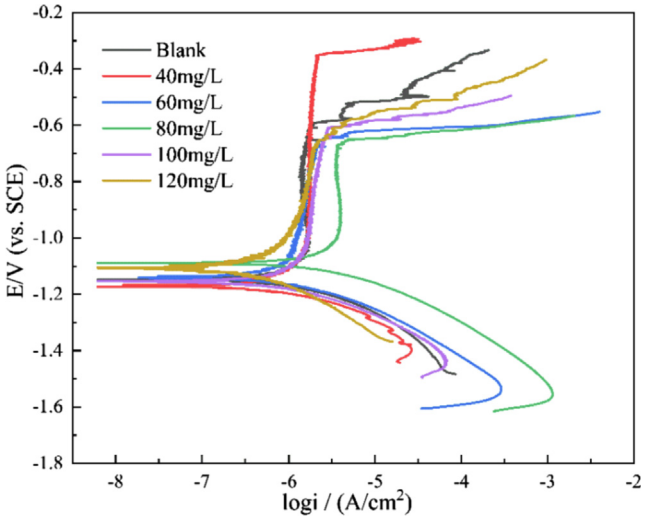

Fig. 4 Polarization curves of 7B04 aluminum alloy immersed in different systems.

Table 1 Electrochemical parameters obtained by polarization curve fitting.

C_{DDBAC} (mg/L)	i_{corr} (μA·cm^2)	E_{corr} (mV vs SCE)	η (%)
0	0.623	−1139	–
40	0.298	−1170	52.17
60	0.219	−1144	64.85
80	0.197	−1096	68.38
100	0.213	−1091	65.81
120	0.225	−1142	63.88

Two time constants are evident in the Bode plot, as seen in Fig. 5, and the one in the high frequency region suggests the formation of an oxide layer on the aluminum alloy surface (Shen et al., 2020). The wide phase angle peak revealed that the oxide film had a certain corrosion resistance. The other time constant at low frequencies could be attributed to the formation of a double electric layer.

An equivalent electrical circuit for the fitting of EIS is established in Fig. 6. In the equivalent circuit, Q is a constant phase element (CPE) and given by:

$$Z_{CPE} = \frac{1}{Y_0(j\omega)^n} \quad (2)$$

where Z_{CPE} is the impedance of CPE, Y_0 is a parameter related to capacitance, j is the unit imaginary number, ω is the angular frequency of the alternating voltage, and n is an exponential term related to the roughness of the electrode surface. R_s represents the solution resistance. R_f and Q_f correspond to the resistance and capacitance of the corrosion film and/or DDBAC adsorption layer, respectively. R_{ct} and Q_{dl} represent the charge transfer resistance and electric double layer capaci-

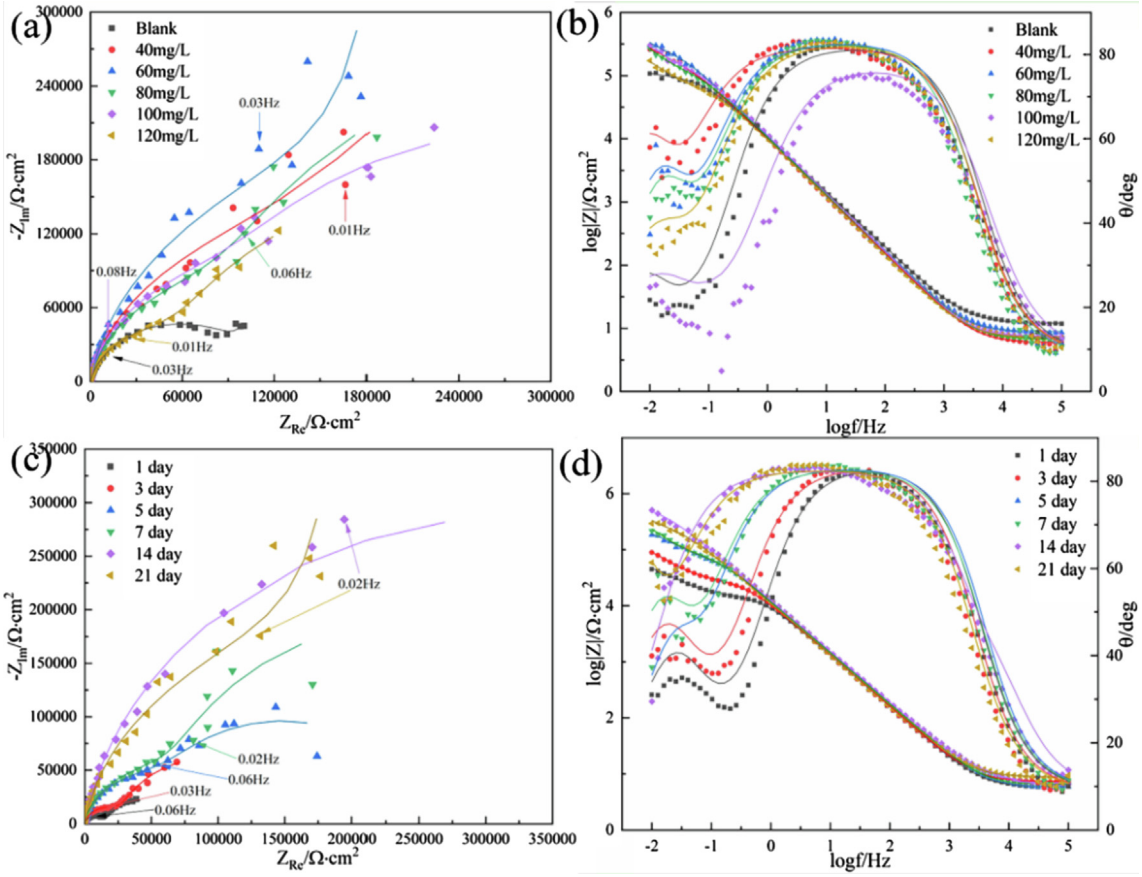

Fig. 5 EIS of 7B04 aluminum alloy immersed in 3.5% NaCl solution with different concentrations of DDBAC for 21 days (a, b) and with 60 mg/L DDBAC over time (c, d).

tance, respectively. Considering the capacitance value, C is proportional to admittance coefficient Y_0,

$$C = \frac{Y_0 \omega^{n-1}}{\sin(n\pi/2)} \tag{3}$$

the latter is used to reflect the relative magnitude relationship of the capacitance. The fitting results are shown in Table 2.

The R_{ct} values in all DDBAC concentration systems were larger than those of the system without DDBAC addition (Table 2), indicating that DDBAC had an inhibitory effect on the corrosion of 7B04 aluminum alloy (Deyab, 2014). In addition, the decrease in Q_{dl} was induced by the decrease in the local dielectric constant and/or the increase in electric double layer thickness. This behavior indicates that DDBAC molecules displace water molecules and other ions which are originally adsorbed at the metal/solution interface (Deyab et al., 2016). Consequently, the protective layer adsorbed at the aluminum alloy surface slows down the dissolution process

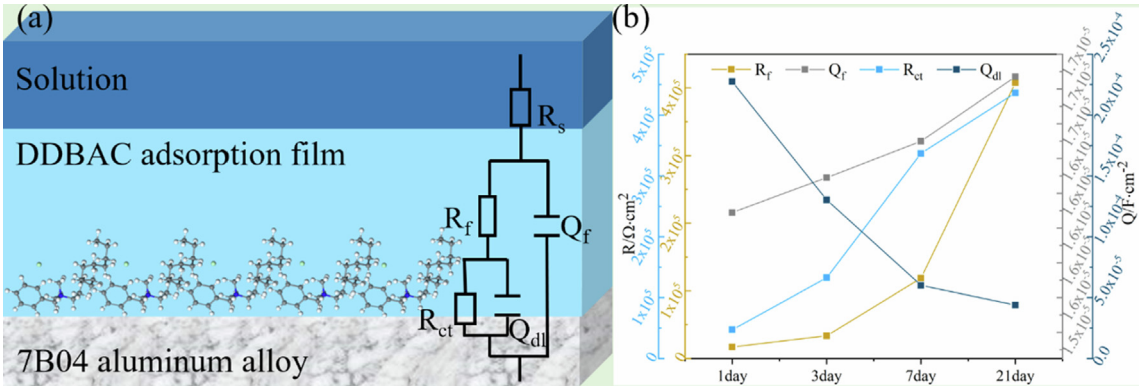

Fig. 6 The equivalent circuit for the fitting of EIS (a) and the fitting results for 7B04 aluminum alloy immersed in 60 mg/L DDBAC over time (b).

of the aluminum alloy. Indeed, the largest effect is obtained with the addition of the 80 mg/L DDBAC which gives an R_{ct} value equal to 443 kΩ·cm^2. Compared with the system absence of DDBAC, Table 2 also clearly shows that the increase of the 'n' value suggests the decrease of surface inhomogeneity, due to the DDBAC molecules adsorbed on the active adsorption sites at the aluminum alloy surface (see Table 3).

Given that the reciprocal of the charge transfer resistance (R_{ct}^{-1}) corresponds to the corrosion rate of metal in corrosive solutions (Deyab et al., 2017), the inhibition efficiency (η) of DDBAC could be calculated using the following equation:

$$\eta = \frac{(R_{ct} + R_f) - (R_{ct}^0 + R_f^0)}{R_{ct} + R_f} \times 100\% \quad (4)$$

where R_{ct}^0 and R_{ct} are charge transfer resistance values in the absence and presence of an inhibitor, respectively.

The values calculated from Eq. (4) are presented in Table 2. The maximum inhibition efficiency was obtained at 60 mg/L after the 21-day immersion. DDBAC had a certain inhibitory effect on aluminum alloy. Meanwhile, Fig. 6 illustrates that R_{ct} gradually increased in the system with 60 mg/L DDBAC within 21 days, revealing that the inhibition effect of DDBAC on 7B04 aluminum alloy increased with time.

3.5. Adsorption isotherm

The adsorption isotherm is very significant for evaluating the adsorption mechanism of the electrochemical reaction between DDBAC and aluminum alloy (Obot et al., 2015). In this study, Temkin, Frumkin, and Langmuir adsorption isotherms were used for the electrochemical polarization data fitting to discuss the mechanism of DDBAC adsorption onto the aluminum/solution interface, which were calculated by the following equations (Xiong et al., 2021):

Langmuir:

$$\frac{C_{inh}}{\theta} = \frac{1}{K_{ads}} + C_{inh} \quad (5)$$

Temkin:

$$\exp(f\theta) = K_{ads}C_{inh} \quad (6)$$

Frumkin:

$$\frac{\theta}{1-\theta}\exp(-2f\theta) = K_{ads}C_{inh} \quad (7)$$

where C_{inh} is the concentration, K_{ads} is the equilibrium constant for the adsorption/desorption process and θ is the degree of surface coverage. It is found that the experimental data are most consistent with the Langmuir isotherm through calculation. The curve of C_{inh}/θ versus C_{inh} is shown in Fig. 7.

The degree of surface coverage for the DDBAC was obtained from polarization data and could be calculated by the following relationship (Ansari et al., 2016):

$$\theta = \frac{I_{corr}^0 - I_{corr}}{I_{corr}^0} \quad (8)$$

The slope is slightly higher than unity (Fig. 7), which can be due to the interactions between DDBAC molecules and aluminum atoms. Therefore, the DDBAC adsorption on the aluminum surface could be appropriately represented by the modified Langmuir equation (Umoren et al., 2013), which considers the interactions between adsorbed substances and the adsorption heat change with surface coverage, as follows:

$$\frac{C_{inh}}{\theta} = \frac{n}{K_{ads}} + nC_{inh} \quad (9)$$

where n is the slope of the adsorption plot.

According to Eq. (5), K_{ads} can be calculated from the intercept line on the C_{inh}/θ axis. The free energies of the adsorption (ΔG_{ads}°) of DDBAC are determined from K_{ads} by (Tan et al., 2020):

$$\Delta G_{ads}^{\circ} = -RT\ln(55.5K_{ads}) \quad (10)$$

where R is the molar gas constant, T is the absolute temperature and 55.5 is the water concentration in the solution expressed in a molar. The calculated value of ΔG_{ads}° value is −38.46 kJ mol^{-1}. The negative value demonstrates that the surfactant adsorption on the aluminum alloy surface is a spontaneous process and a strong interaction exists between surfactant molecules and the aluminum surface (Okafor and Zheng, 2009).

Importantly, the ΔG_{ads}° value is closely related to the adsorption type. When the value of ΔG_{ads}° is greater than −20 kJ/mol, then the interaction between the surfactant and metal is classified as physisorption (Ramezanzadeh et al., 2019). When the adsorption free energy is less than −40 kJ/mol, then the surface undergoes chemisorption (Biswas et al., 2018). Based on the calculated value of adsorption free energy, −38.46 kJ mol^{-1}, the adsorption mechanism of the DDBAC can be classified as a combination of chemisorption and physisorption.

3.6. Quantum chemical calculations

Quantum chemical calculations were carried out to further investigate the corrosion inhibition mechanism of DDBAC. DFT has been widely used to explore the corrosion inhibition

Table 2 Fitting electrochemical parameters of 7B04 aluminum alloy after immersion in different concentrations of DDBAC for 21 days.

C_{DDBAC} (mg/L)	R_s (Ω·cm^2)	Q_f (F·cm^{-2})	R_f (Ω·cm^{-2})	n_1	Q_{dl} (F·cm^{-2})	R_{ct} (Ω·cm^{-2})	n_2	η (%)
0	12.06	1.87×10^{-5}	1.13×10^{5}	0.8733	4.89×10^{-4}	1.65×10^{5}	0.8042	–
40	5.96	1.90×10^{-5}	2.57×10^{5}	0.9054	4.77×10^{-5}	2.75×10^{5}	0.8647	47.74
60	8.91	1.69×10^{-5}	4.08×10^{5}	0.9116	4.39×10^{-5}	3.86×10^{5}	0.9227	64.99
80	6.66	1.78×10^{-5}	2.47×10^{5}	0.9064	5.69×10^{-5}	4.43×10^{5}	0.8872	59.71
100	7.55	1.60×10^{-5}	2.97×10^{5}	0.9222	5.37×10^{-5}	3.51×10^{5}	0.8869	57.10
120	7.17	1.86×10^{-5}	3.29×10^{5}	0.9136	6.99×10^{-5}	3.24×10^{5}	0.8902	57.43

Table 3 The calculated quantum chemical parameters for DDBAC.

Inhibitor	E_{HOMO}/eV	E_{LUMO}/eV	ΔE/eV	χ/eV	η/eV
DDBAC	−0.129	−0.053	0.076	0.091	0.038

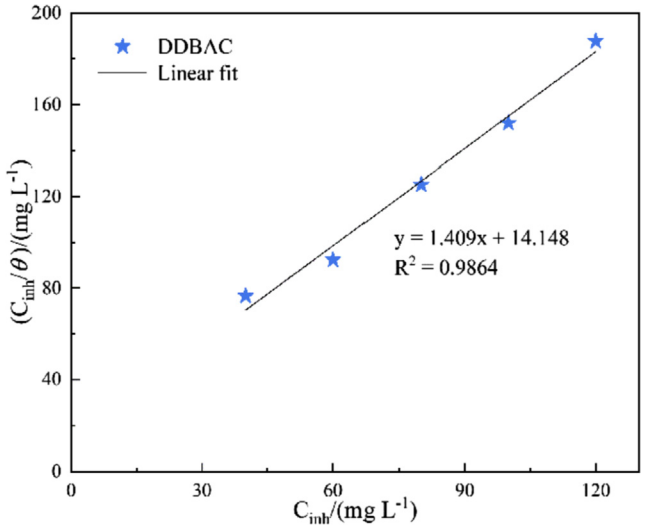

Fig. 7 Langmuir adsorption isotherm of DDBAC on the aluminum alloy surface at 298 K.

mechanism. The corrosion inhibition depends on the electronic and geometric structures of corrosion inhibitor molecules (Singh et al., 2017; Verma et al., 2021). Quantum chemical parameters were used to correlate the experimental studies for the inhibition efficiency of DDBAC and its structural and electronic properties.

The chemical reactivity depends on the interaction between the highest occupied molecular orbital (HOMO) and the lowest unoccupied molecular orbital (LUMO) levels of the reactants (Mai et al., 2019). The HOMO and LUMO electronic density distributions for the DDBAC molecule are shown in the graphical images in Fig. 8. As shown in the figure, the electron density distributions of HOMO regions were focused mainly on nitrogen atoms. Those of LUMO regions were concentrated on nitrogen atoms and benzene rings. Thus, benzene rings and nitrogen atoms were the active parts in the DDBAC molecule. The HOMO and LUMO electronic surfaces revealed that the DDBAC molecule could the potential to donate and accept electrons under favorable conditions (Errahmany et al., 2020; Manssouri et al., 2020). It is supposed to be the main reason for DDBAC adsorption on aluminum alloy. The Energy gap (ΔE) represents the adsorption tendency of the corrosion inhibitor on the metal interface. The adsorption ability of the corrosion inhibitor on the steel surface increased as ΔE decreased.

The electronegativity (χ) and the global hardness (η) of the inhibitor molecules are as follows:

$$\chi = \frac{-E_{HOMO} - E_{LUMO}}{2} \tag{11}$$

$$\eta = \frac{E_{LUMO} - E_{HOMO}}{2} \tag{12}$$

As shown in Table 3, the values of E_{HOMO}, E_{LUMO}, and ΔE were −0.129, −0.053, and 0.076 eV respectively, indicating that DDBAC had excellent adsorption ability and corrosion inhibition efficiency.

Fig. 9 shows the Mulliken charges of the heteroatoms in the DDBAC molecule. The electron density distribution in the molecule directly affects the corrosion inhibitor adsorption on the metal surface. In general, the electrophilic groups first attack the locations where the negative charges are concentrated in the corrosion inhibitor molecules. These locations are the active centers where the corrosion inhibitor molecules are adsorbed. In Fig. 9, the highest negative charge was located on the nitrogen atom with a value of −0.382 eV. Therefore, the nitrogen atom readily supplies electrons to the metal aluminum atom and can bind with the aluminum atom. It is the active position for interaction with the aluminum alloy. That is, the adsorption process may occur through nitrogen atoms in the DDBAC molecule.

MEP is important for mapping the molecule surface and used to predict the most active site of proximity and/or reaction with other molecules on the basis of the charge and electron distributions on the molecule surface (Abd El-Lateef and Alnajjar, 2020). When two molecules are in close proximity, MEP plays a key role in the approach mode, as the electrophilic reagents always attack the most negative site. Fig. 10 displays the MEP of the DDBAC molecule with the maximum value located at the nitrogen atom. Combined with the charge distributions of HOMO, LUMO, and Mulliken, nitrogen atoms are proven to be the active center adsorbed on the metal surface. The results obtained from quantum chemical studies are in accordance with the experimental results.

4. Discussions

Considering that the cell surfaces of bacteria are generally negatively charged, the higher the positive charge density in the

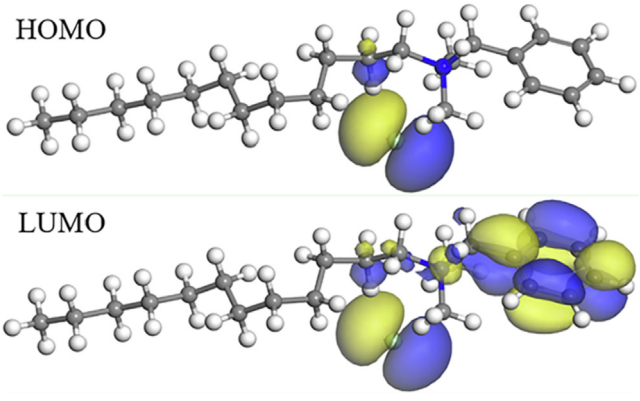

Fig. 8 HOMO density distribution and the LUMO density distribution for DDBAC molecule obtained with DFT.

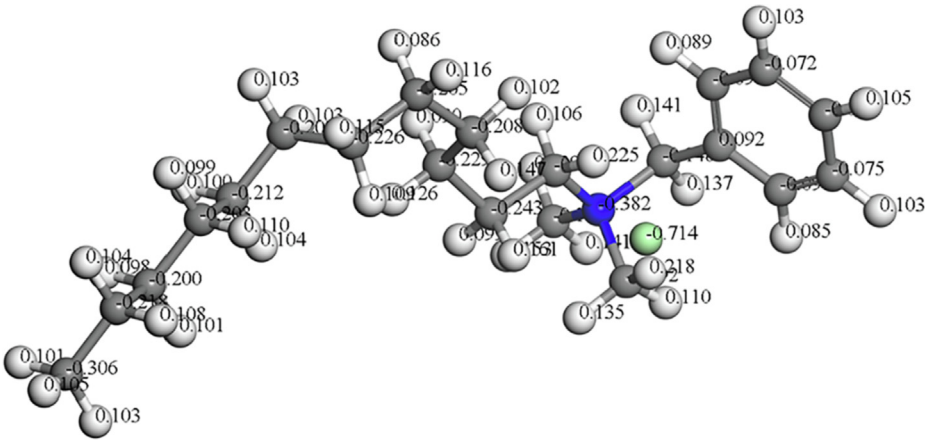

Fig. 9 Mulliken atomic charges calculated for DDBAC molecule.

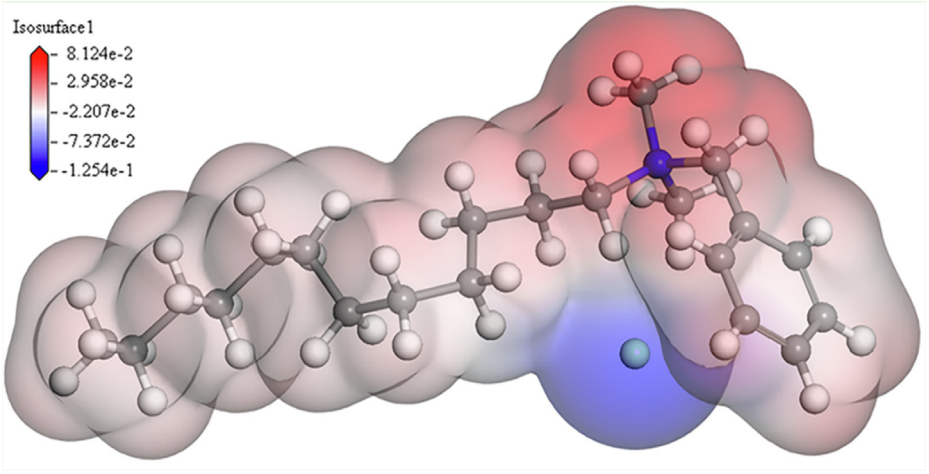

Fig. 10 The MEP surfaces of the DDBAC.

molecule of cationic bactericide, the better the ability to adsorb on the cell surface (Vieira and Carmona-Ribeiro, 2006); the more positive charges adsorbed on the bacterial surface, the better the effect on cell wall permeability alteration and membrane disruption, and the easier it is for intracellular components of the bacteria to leak out and die (Campanhã et al., 1999). As displayed in Fig. 11, the antimicrobial activity of DDBAC is due to the adsorption of positively charged quaternary ammonium ions onto the surface of negatively charged *L. sphaericus*, *A. lwoffii*, and *S. salmoneum*, thus altering cell wall permeability. Moreover, the DDBAC molecular chain contains dodecyl. According to the relationship between antimicrobial ability and the toxicity of quaternary ammonium salt and its structure, the alkyl chain has strong membrane affinity and a good antimicrobial effect when the number of carbon atoms is 10–16 (Lincopan et al., 2005). Due to the good flocculation and sedimentation effect of DDBAC, microorganisms are effectively concentrated in the sediment through flocculation. It is beneficial for the concentrated killing of microorganisms and enables DDBAC a good antimicrobial activity (Singh et al., 2018).

Fig. 12 reveals that DDBAC molecules form a chemisorbed layer on the aluminum alloy surface. As seen from Figs. 8–10, the nitrogen atom in DDBAC molecule provided a lone pair of electrons, which coordinated and combined with metal atoms to form a solid chemisorption layer. In addition, the benzene ring could be chemisorbed on the metal surface through the action of π bonds, resulting in the formation of stable complexes between the DDBAC and the metal (Luo et al., 2019). DDBAC was combined with the active sites on the aluminum alloy to prevent from the corrosion reaction. The inhibition mechanism is explained by reaction formula (13):

$$Al + DDBAC \rightarrow Al - DDBAC_{(ads)} \tag{13}$$

The strength of the bond between the adsorbed layer and the metal depends on the adsorption properties and the strength of the chemical bond between them (Luo et al., 2017). In addition, the nonpolar group of the DDBAC molecule is hydrophobic. It is located in the direction away from the metal and acts as a barrier through the water-repellent base to separate the metal surface from the corrosive medium

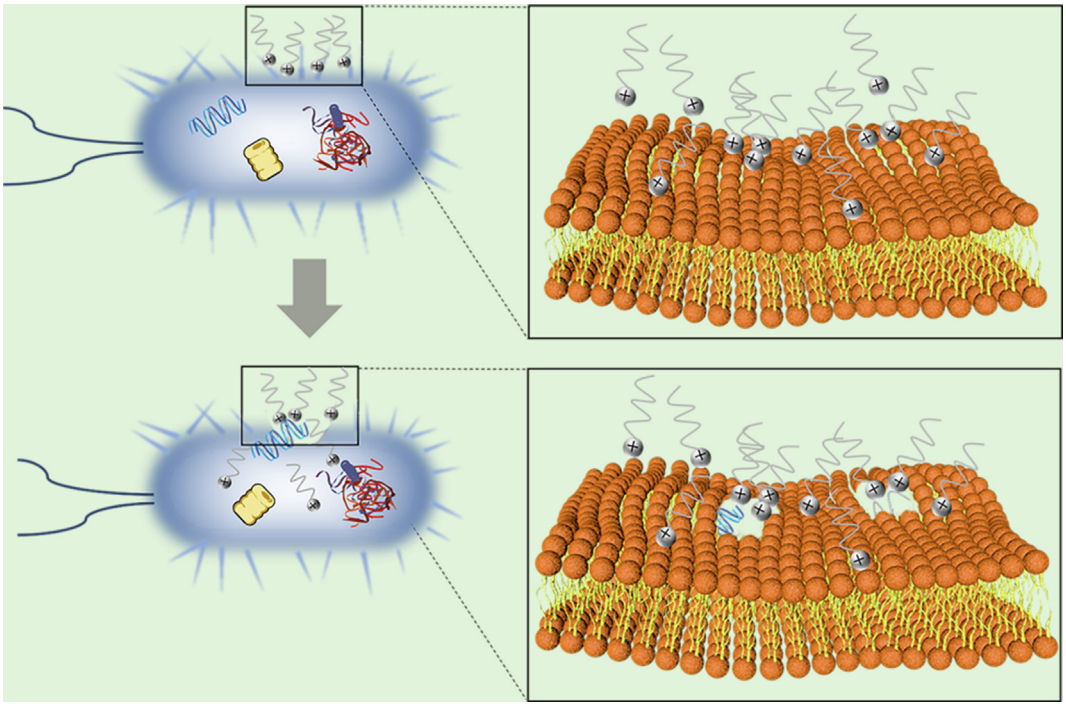

Fig. 11 Antimicrobial mechanism diagram of DDBAC.

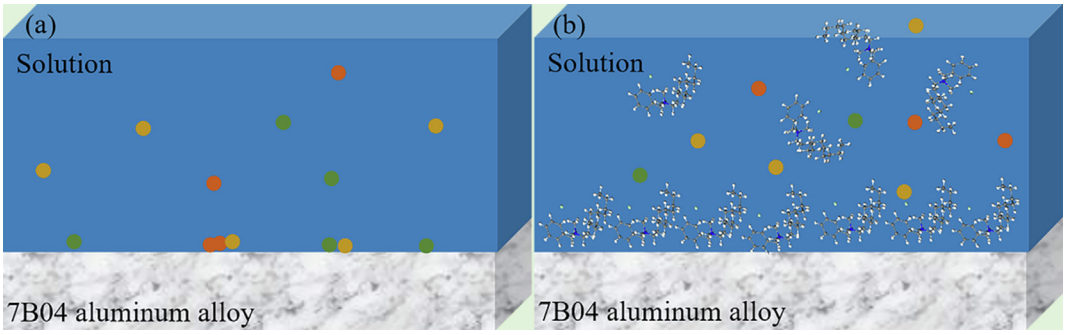

Fig. 12 Corrosion inhibition mechanism diagram of DDBAC.

(Ramezanzadeh et al., 2019). Thus, a physical barrier is formed between the metal and the solution to reduce the corrosion.

5. Conclusions

Microbiologically influenced corrosion is an important problem for naval aircraft. In this study, the antimicrobial ability of DDBAC on contaminative microorganisms in naval aircraft fuel systems was evaluated by the inhibition zone method and minimum inhibitory concentration test. The effect of DDBAC on the corrosion of fuel tank material was investigated by polarization curve and EIS. The quantum chemical calculation was carried out to study the correlation between the inhibitory effect and molecular structure of DDBAC. The results showed that DDBAC had an antimicrobial performance for *S. salmoneum, A. lwoffii,* and *L. sphaericus* isolated and purified from the navy aircraft fuel system. Moreover, the minimum inhibitory concentration of DDBAC was 64 mg/L. The polarization curve indicated that DDBAC acted as a mixed-type inhibitor that suppressed both anodic and cathodic reactions. The impedance results showed that DDBAC formed an adsorption layer on the aluminum alloy surface to prevent the charge transfer. The metal corrosion process was inhibited by the DDBAC adsorption on the aluminum alloy surface and its adsorption fitted the modified Langmuir adsorption isotherm model. The corresponding value of ΔG°_{ads} revealed that the adsorption mechanism of the DDBAC could be classified as a combination of chemisorption and physisorption. A good consistency among the experimental and DFT results were also observed. The lone pair of electrons of nitrogen atoms in DDBAC were able to form coordinate bonds with the empty orbital in the aluminum alloy, resulting in a tight chemisorption layer and corrosion inhibition.

CRediT authorship contribution statement

Shuai Wang: Data curation, Formal analysis, Writing-original draft. **Jie Sun:** Data curation, Investigation. **Borong Shan:**

Investigation, Software. **Weijie Fan:** Funding acquisition, Supervision, Validation. **Rui Ding:** Methodology, Software. **Jie Yang:** Validation, Resources. **Xiaodong Zhao:** Conceptualization, Funding acquisition, Writing-review & editing.

Declaration of Competing Interest

The authors declare that they have no known competing financial interests or personal relationships that could have appeared to influence the work reported in this paper.

Acknowledgements

The work was supported by State Key Laboratory of Ocean Engineering (Shanghai Jiao Tong University) (Grant No. 1912), Graduate Innovation Foundation of Yantai University, GIFYTU (No. YDYB2107) and the Green innovation science and technology plan of colleges and universities in Shandong Province (No. 2020KJA014).

References

Abd-Elaal, A.A., Shaban, S.M., Tawfik, S.M., 2017. Three gemini cationic surfactants based on polyethylene glycol as effective corrosion inhibitor for mild steel in acidic environment. J. Associa. Arab. Univer. Basic. Appl. Sci. 24, 54–65. https://doi.org/10.1016/j.jaubas.2017.03.004.

Abd El-Lateef, H.M., Alnajjar, A.O., 2020. Enhanced the protection capacity of poly(o-toluidine) by synergism with zinc or lanthanum additives at C-steel/HCl interface: A combined DFT, molecular dynamic simulations and experimental methods. J. Mol. Liq. 303,. https://doi.org/10.1016/j.molliq.2020.112641 112641.

Ansari, K.R., Quraishi, M.A., Singh, A., Ramkumar, S., 2016. Corrosion inhibition of N80 steel in 15% HCl by pyrazolone derivatives: electrochemical, surface and quantum chemical studies. Rsc. Adv. 6, 24130–24141. https://doi.org/10.1039/c5ra25441h.

Biswas, A., Mourya, P., Mondal, D., Pal, S., 2018. Grafting effect of gum acacia on mild steel corrosion in acidic medium: Gravimetric and electrochemical study. J. Mol. Liq. 251, 470–479. https://doi.org/10.1016/j.molliq.2017.12.087.

Brown, L.M., Mccomb, J.P., Vangsness, M.D., Bowen, L.L., 2010. Community dynamics and phylogenetics of bacteria fouling Jet A and JP-8 aviation fuel. Int. Biodeter. Biodegr. 64, 253–261. https://doi.org/10.1016/j.ibiod.2010.01.008.

Bücker, F., Barbosa, C.S., Quadros, P.D., Bueno, M.K., 2014. Fuel biodegradation and molecular characterization of microbial biofilms in stored diesel/biodiesel blend B10 and the effect of biocide. Int. Biodeter. Biodegr. 95, 346–355. https://doi.org/10.1016/j.ibiod.2014.05.030.

Campanhã, M.T.N., Mamizuka, E.M., Carmona-Ribeiro, A.M., 1999. Interactions between cationic liposomes and bacteria: the physical-chemistry of the bactericidal action. J. Lipid. Res. 40, 1495–1500. https://doi.org/10.1016/s0022-2275(20)33392-7.

Chowdhuri, A.R., Das, B., Kumar, A., Tripathy, S., 2017. One-pot synthesis of multifunctional nanoscale metal-organic frameworks as an effective antibacterial agent against multidrug-resistant staphylococcus aureus. Nanotechnology. 28, 95–102. https://doi.org/10.1088/1361-6528/aa57af.

Cui, Q., Liu, T., Li, X., Zhao, L., 2021. Validation of the mechano-bactericidal mechanism of nanostructured surfaces with finite element simulation. Colloid. Surface. B. 206,. https://doi.org/10.1016/j.colsurfb.2021.111929 111929.

Deyab, M.A., 2014. Corrosion protection of aluminum bipolar plates with polyaniline coating containing carbon nanotubes in acidic medium inside the polymer electrolyte membrane fuel cell. J. Power. Sources. 268, 50–55. https://doi.org/10.1016/j.jpowsour.2014.06.021.

Deyab, M.A., 2018. Efficiency of cationic surfactant as microbial corrosion inhibitor for carbon steel in oilfield saline water. J. Mol. Liq. 255, 550–555. https://doi.org/10.1016/j.molliq.2018.02.019.

Deyab, M.A., Essehli, R., El Bali, B., Lachkar, M., 2017. Fabrication and evaluation of $Rb_2Co(H_2P_2O_7)_2{\cdot}2H_2O$/waterborne polyurethane nanocomposite coating for corrosion protection aspects. Rsc. Adv. 7, 55074–55080. https://doi.org/10.1039/c7ra11212b.

Deyab, M.A., Ouarsal, R., Lachkar, M., 2016. Phosphites compound: Novel corrosion inhibitor for radioactive waste container (carbon steel) in simulated Callovo-Oxfordian (C_Ox) groundwater. J. Mol. Liq. 219, 994–999. https://doi.org/10.1016/j.molliq.2016.04.027.

Ding, M., He, X., Wang, Z., Li, J., 2011. Cellular uptake of polyurethane nanocarriers mediated by gemini quaternary ammonium. Biomaterials. 32, 9515–9524. https://doi.org/10.1016/j.biomaterials.2011.08.074.

Errahmany, N., Rbaa, M., Abousalem, A.S., Tazouti, A., 2020. Experimental, DFT calculations and MC simulations concept of novel quinazolinone derivatives as corrosion inhibitor for mild steel in 1.0 M HCl medium. J. Mol. Liq. 312,. https://doi.org/10.1016/j.molliq.2020.113413 113413.

Finšgar, M., Jackson, J., 2014. Application of corrosion inhibitors for steels in acidic media for the oil and gas industry: A review. Corros. Sci. 86, 17–41. https://doi.org/10.1016/j.corsci.2014.04.044.

Gu, J., Yuan, L., Zhang, Z., Yang, X., 2018. Non-leaching bactericidal cotton fabrics with well-preserved physical properties, no skin irritation and no toxicity. Cellulose. 25, 5415–5426. https://doi.org/10.1007/s10570-018-1943-8.

Hsissou, R., Benhiba, F., Dagdag, O., 2020. Development and potential performance of prepolymer in corrosion inhibition for carbon steel in 1.0 M HCl: Outlooks from experimental and computational investigations. J. Colloid. Interface. Sci. 574, 43–60. https://doi.org/10.1016/j.jcis.2020.04.022.

Jennings, M.C., Minbiole, K.P., Wuest, W.M., 2015. Quaternary ammonium compounds: an antimicrobial mainstay and platform for innovation to address bacterial resistance. Acs. Infect. Dis. 1, 288–303. https://doi.org/10.1021/acsinfecdis.5b00047.

Karn, S.K., Fang, G., Duan, J., 2017. *Bacillus sp*. acting as dual role for corrosion induction and corrosion inhibition with carbon steel (CS). Front. Microbiol. 8, 2038. https://doi.org/10.3389/fmicb.2017.02038.

Krishnaveni, K., Ravichandran, J., 2014. Effect of aqueous extract of leaves of Morinda tinctoria on corrosion inhibition of aluminium surface in HCl medium. T. Nonferr. Metal. Soc. 24, 2704–2712. https://doi.org/10.1016/s1003-6326(14)63401-4.

Li, X.D., Wang, X.S., Ren, H.H., Chen, Y.L., 2012. Effect of prior corrosion state on the fatigue small cracking behaviour of 6151–T6 aluminum alloy. Corros. Sci. 55, 26–33. https://doi.org/10.1016/j.corsci.2011.09.025.

Lincopan, N., Mamizuka, E.M., Carmona-Ribeiro, A.M., 2005. Low nephrotoxicity of an effective amphotericin B formulation with cationic bilayer fragments. J. Antimicrob. Chemother. 55, 727–734. https://doi.org/10.1093/jac/dki064.

Liu, H., Gu, T., Lv, Y., Asif, M., 2017. Corrosion inhibition and antibacterial efficacy of benzalkonium chloride in artificial CO_2-saturated oilfield produced water. Corro. Sci. 117, 24–34. https://doi.org/10.1016/j.corsci.2017.01.006.

Liu, X., Li, Z., Fan, Y., Lekbach, Y., 2020. A mixture of D-Amino acids enhances the biocidal efficacy of CMIT/MIT against corrosive *Vibrio harveyi* biofilm. Front. Microbiol. 11,. https://doi.org/10.3389/fmicb.2020.557435 557435.

Luo, X., Ci, C., Li, J., Lin, K., 2019. 4-aminoazobenzene modified natural glucomannan as a green eco-friendly inhibitor for the mild steel in 0.5 M HCl solution. Corros. Sci. 151, 132–142. https://doi.org/10.1016/j.corsci.2019.02.027.

Luo, X., Pan, X., Yuan, S., Du, S., 2017. Corrosion inhibition of mild steel in simulated seawater solution by a green eco-friendly mixture

of glucomannan (GL) and bisquaternary ammonium salt (BQAS). Corros. Sci. 125, 139–151. https://doi.org/10.1016/j.corsci.2017.06.013.

Mai, M.K., Tantawy, A.H., Soliman, K.A., El-Lateef, H., 2019. Cationic Gemini-surfactants based on waste cooking oil as New 'Green' inhibitors for N80-steel corrosion in sulphuric acid: A Combined Empirical and Theoretical Approaches. J. Mol. Struct. 1203,. https://doi.org/10.1016/j.molstruc.2019.127442 127442.

Manssouri, M., Znini, M., Lakbaibi, Z., Ansari, A., 2020. Experimental and computational studies of perillaldehyde isolated from *Ammodaucus leucotrichus* essential oil as a green corrosion inhibitor for mild steel in 1.0 M HCl. Chem. Pap. 75, 1103–1114. https://doi.org/10.1007/s11696-020-01353-5.

Migahed, M.A., Hegazy, M.A., Al-Sabagh, A.M., 2012. Synergistic inhibition effect between Cu^{2+} and cationic gemini surfactant on the corrosion of downhole tubing steel during secondary oil recovery of old wells. Corros. Sci. 61, 10–18. https://doi.org/10.1016/j.corsci.2012.04.004.

Obot, I.B., Umoren, S.A., Gasem, Z.M., Suleiman, R., 2015. Theoretical prediction and electrochemical evaluation of vinylimidazole and allylimidazole as corrosion inhibitors for mild steel in 1 M HCl. J. Ind. Eng. Chem. 21, 1328–1339. https://doi.org/10.1016/j.jiec.2014.05.049.

Okafor, P.C., Zheng, Y., 2009. Synergistic inhibition behaviour of methylbenzyl quaternary imidazoline derivative and iodide ions on mild steel in H_2SO_4 solutions. Corros. Sci. 51, 850–859. https://doi.org/10.1016/j.corsci.2009.01.027.

Pantelakis, S.G., Chamos, A.N., Setsika, D., 2012. Tolerable corrosion damage on aircraft aluminum structures: Local cladding patterns. Theor. Appl. Fract. Mec. 58, 55–64. https://doi.org/10.1016/j.tafmec.2012.02.008.

Passman, F.J., 2013. Microbial contamination and its control in fuels and fuel systems since 1980-a review. Int. Biodeter. Biodegr. 81, 88–104. https://doi.org/10.1016/j.ibiod.2012.08.002.

Ramezanzadeh, M., Bahlakeh, G., Sanaei, Z., Ramezanzadeh, B., 2019. Corrosion inhibition of mild steel in 1 M HCl solution by ethanolic extract of eco-friendly Mangifera indica (mango) leaves: Electrochemical, molecular dynamics, Monte Carlo and ab initio study. Appl. Surf. Sci. 463, 1058–1077. https://doi.org/10.1016/j.apsusc.2018.09.029.

Samy, M., Shaban, I., Aiad, M., 2015. Preparation of capped silver nanoparticles using sunlight and cationic surfactants and their biological activity. Chinese. Chem. Lett. 26, 1415–1420. https://doi.org/10.1016/j.cclet.2015.06.006.

Shaban, S.M., Aiad, I., El-Sukkary, M.M., 2015. Surface and biological activity of N-(((dimethoxybenzylidene)amino)propyl)-N, N-dimethylalkyl-1-ammonium derivatives as cationic surfactants. J. Mol. Liq. 207, 256–265. https://doi.org/10.1016/j.molliq.2015.03.043.

Shen, Y., Dong, Y., Yang, Y., Li, Q., 2020. Study of pitting corrosion inhibition effect on aluminum alloy in seawater by biomineralized film. Bioelectrochemistry. 132,. https://doi.org/10.1016/j.bioelechem.2019.107408 107408.

Shi, L., He, Y., Lu, J., Liang, D., 2020. Effect of dodecyl dimethyl benzyl ammonium chloride on CH_4 hydrate growth and agglomeration in oil-water systems. Energy. 212,. https://doi.org/10.1016/j.energy.2020.118746 118746.

Singh, A., Ansari, K.R., Haque, J., Dohare, P., 2018. Effect of electron donating functional groups on corrosion inhibition of mild steel in hydrochloric acid: Experimental and quantum chemical study. J. Taiwan. Inst. E. 82, 233–251. https://doi.org/10.1016/j.jtice.2017.09.021.

Singh, A., Ansari, K.R., Kumar, A., Liu, W., 2017. Electrochemical, surface and quantum chemical studies of novel imidazole derivatives as corrosion inhibitors for J55 steel in sweet corrosive environment. J. Alloy. Compo. 712, 121–133. https://doi.org/10.1016/j.jallcom.2017.04.072.

Sylvie, B.-B., Pierre, T., 2012. Emergence of resistance to antibacterial agents: the role of quaternary ammonium compounds-a critical review. Int. J. Antimicrob. Ag. 39, 381–389. https://doi.org/10.1016/j.ijantimicag.2012.01.011.

Tan, B., Xiang, B., Zhang, S., Qiang, Y., 2021. Papaya leaves extract as a novel eco-friendly corrosion inhibitor for Cu in H_2SO_4 medium. J. Colloid. Interf. Sci. 582, 918–931. https://doi.org/10.1016/j.jcis.2020.08.093.

Tan, B., Zhang, S., Qiang, Y., Li, W., 2020. Experimental and theoretical studies on the inhibition properties of three diphenyl disulfide derivatives on copper corrosion in acid medium. J. Mol. Liq. 298,. https://doi.org/10.1016/j.molliq.2019.111975 111975.

Umoren, S.A., Banera, M.J., Alonso-Garcia, T., Gervasi, C.A., 2013. Inhibition of mild steel corrosion in HCl solution using chitosan. Cellulose. 20, 2529–2545. https://doi.org/10.1007/s10570-013-0021-5.

Verma, C., Ebenso, E.E., Quraishi, M.A., 2020. Molecular structural aspects of organic corrosion inhibitors: influence of -CN and -NO_2 substituents on designing of potential corrosion inhibitors for aqueous media. J. Mol. Liq. 316,. https://doi.org/10.1016/j.molliq.2020.113874 113874.

Verma, D.K., Kaya, S., Ech-Chihbi, E., 2021. Investigations on some coumarin based corrosion inhibitors for mild steel in aqueous acidic medium: Electrochemical, surface morphological, density functional theory and Monte Carlo simulation approach. J. Mol. Liq. 329,. https://doi.org/10.1016/j.molliq.2021.115531 115531.

Vieira, D.B., Carmona-Ribeiro, A.M., 2006. Cationic lipids and surfactants as antifungal agents: mode of action. J. Antimicrob. Chemo. Th. 58, 760–767. https://doi.org/10.1093/jac/dkl312.

Wang, S., Zhao, X., Rong, H., 2022. Role of *Lysinibacillus sphaericus* on aviation kerosene degradation and corrosion of 7B04 aluminum alloy. J. Mater. Res. Technol. 18, 2641–2653.

Wang, X., Hu, H., Zhao, X., Chen, M., 2019. Novel quinazolin-4(3H)-one derivatives containing a 1,3,4-oxadiazole thioether moiety as potential bactericides and fungicides: Design, synthesis, characterization and 3D-QSAR analysis. J. Saudi. Chem. Soc. 23, 1144–1156. https://doi.org/10.1016/j.jscs.2019.07.006.

Xiong, L., Wang, P., He, Z., Chen, Q., 2021. Corrosion behaviors of Q235 carbon steel under imidazoline derivatives as corrosion inhibitors: Experimental and computational investigations. Arab. J. Chem. 14,. https://doi.org/10.1016/j.arabjc.2020.102952 102952.

Xue, Y., Xiao, H., Zhang, Y., 2015. Antimicrobial polymeric materials with quaternary ammonium and phosphonium salts. Int. J. Mol. Sci. 16, 3626–3655. https://doi.org/10.3390/ijms16023626.

Yadav, M., Gope, L., Kumari, N., Yadav, P., 2016. Corrosion inhibition performance of pyranopyrazole derivatives for mild steel in HCl solution: Gravimetric, electrochemical and DFT studies. J. Mol. Liq. 216, 78–86. https://doi.org/10.1016/j.molliq.2015.12.106.

Zhang, T., Gu, J., Liu, X., Wei, D., 2020a. Bactericidal and antifouling electrospun PVA nanofibers modified with a quaternary ammonium salt and zwitterionic sulfopropylbetaine. Mater. Sci. Eng. C. Mater. Biol. Appl. 111,. https://doi.org/10.1016/j.msec.2020.110855 110855.

Zhang, W., Wu, Y.C., Li, H.J., 2020b. Apostichopus japonicus polysaccharide as efficient sustainable inhibitor for mild steel against hydrochloric acid corrosion. J. Mol. Liq. 321,. https://doi.org/10.1016/j.molliq.2020.114923 114923.

Zhang, Y., He, X., Ding, M., He, W., 2018. Antibacterial and biocompatible crosslinked waterborne polyurethanes containing gemini quaternary ammonium salts. Biomacromolecules. 19, 279–287. https://doi.org/10.1021/acs.biomac.7b01016.

Zhu, Y., Free, M.L., Yi, G., 2015a. Electrochemical measurement, modeling, and prediction of corrosion inhibition efficiency of ternary mixtures of homologous surfactants in salt solution. Corros. Sci. 98, 417–429. https://doi.org/10.1016/j.corsci.2015.05.050.

Zhu, Y., Free, M.L., Yi, G., 2015b. Experimental investigation and modeling of the performance of pure and mixed surfactant

inhibitors: Aggregation, Adsorption, and Corrosion Inhibition on Steel Pipe in Aqueous Phase. J. Electrochem. Soc. 162, 582–591. https://doi.org/10.1149/2.09415010jes.

Zhu, Y., Free, M.L., Yi, G., 2016. The effects of surfactant concentration, adsorption, aggregation, and solution conditions on steel corrosion inhibition and associated modeling in aqueous media. Corros. Sci. 102, 233–250. https://doi.org/10.1016/j.corsci.2015.10.012.